Electronic Supplementary Information

Redox dynamics of 2D crystalline vanadium oxide phases on high-index anatase facets

Martin Ek[1,2,3], Anita Godiksen[1], Logi Arnarson[1], Poul Georg Moses[1], Søren B. Rasmussen[1], Magnus Skoglundh[4], Eva Olsson[2], and Stig Helveg[*5]

[1] Topsoe A/S, Haldor Topsøes Allé 1, DK-2800 Kgs. Lyngby, Denmark

[2] Competence Centre for Catalysis, and Department of Physics, Chalmers University of Technology, 41296 Göteborg, Sweden

[3] Centre for Analysis and Synthesis, Lund University, Box 124, Lund 22100, Sweden

[4] Competence Centre for Catalysis, and Department of Chemistry and Chemical Engineering, Chalmers University of Technology, 41296 Göteborg, Sweden

[5] Center for Visualizing Catalytic Processes (VISION), Department of Physics, Technical University of Denmark, DK-2800 Kgs. Lyngby, Denmark

*E-mail: stig@fysik.dtu.dk

Supplementary Figures

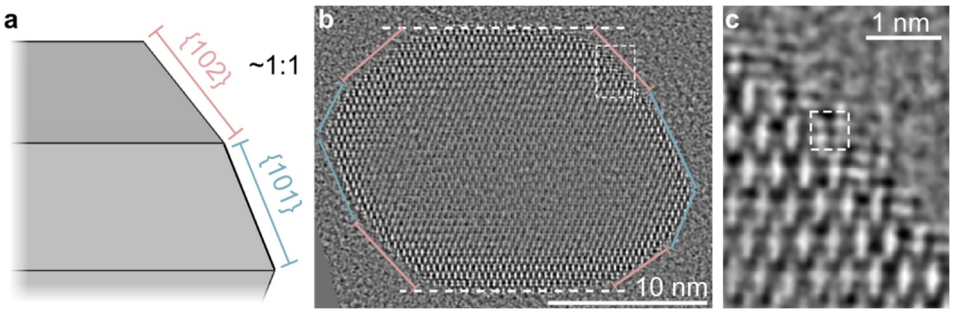

Supplementary Figure S1. Justification for the average particle shape and faceting. (**a**) Detail of the model in Figure 1a in the main text, and Supplementary Figure S3, showing the approximately equal projected extension of the {101} and {102} facets along the perimeter of the particle, when viewed in a [010] orientation. The average diameters of 39 nm and 24 nm along ⟨101⟩ and ⟨001⟩ directions, respectively, are calculated based on the broadening of the corresponding reflections in the powder X-ray diffraction pattern (see reference 17 in the main text). Since ⟨102⟩ is just a linear combination of ⟨101⟩ and ⟨001⟩ directions, the corresponding diameter and {102} area cannot be independently evaluated using this method. Instead, we note that the projected extensions of {101} and {102} in multiple particles are roughly equal: e.g., 18 nm and 20 nm respectively for the particle shown in the exit wave phase image in (**b**). (**c**) Cropped area from the {102} facet showing the cubic motif of rock-salt VO arising due to vacuum reduction at 300 °C.

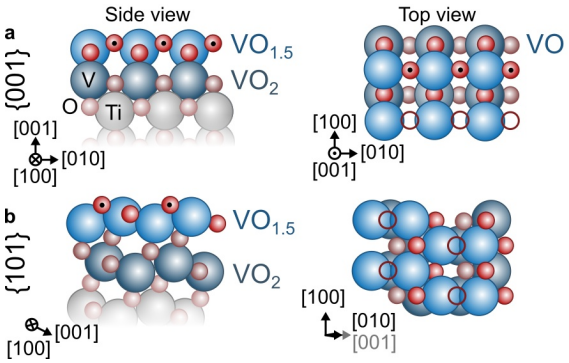

Supplementary Figure S2. Reduction processes illustrated for bulk truncation models of 2 monolayer VO_x/TiO_2, shown in side view prior to reduction and in top view post reduction for (**a**) {001} and (**b**) {101} surfaces. In both cases, one twofold coordinated oxygen atom can be removed per vanadium atom on average (indicated by • in the side view). This results in surface layers with $VO_{1.5}$ compositions on top of an (unchanged) VO_2 layer for a total average of $VO_{1.75}$, as shown in the top view (where empty circles indicate the removed oxygen atoms). For the {001} surface, there would have been additional twofold oxygen atoms to remove in the absence of reconstruction of the vanadium sub-lattice (indicated by • in the top view) – but this is not the case as described in ref. 16. However, even in this case the total average is still limited to $VO_{1.5}$, i.e. the average oxidation state over the nanoparticles should be limited to the V(III)-V(IV) range in mildly reducing environments.

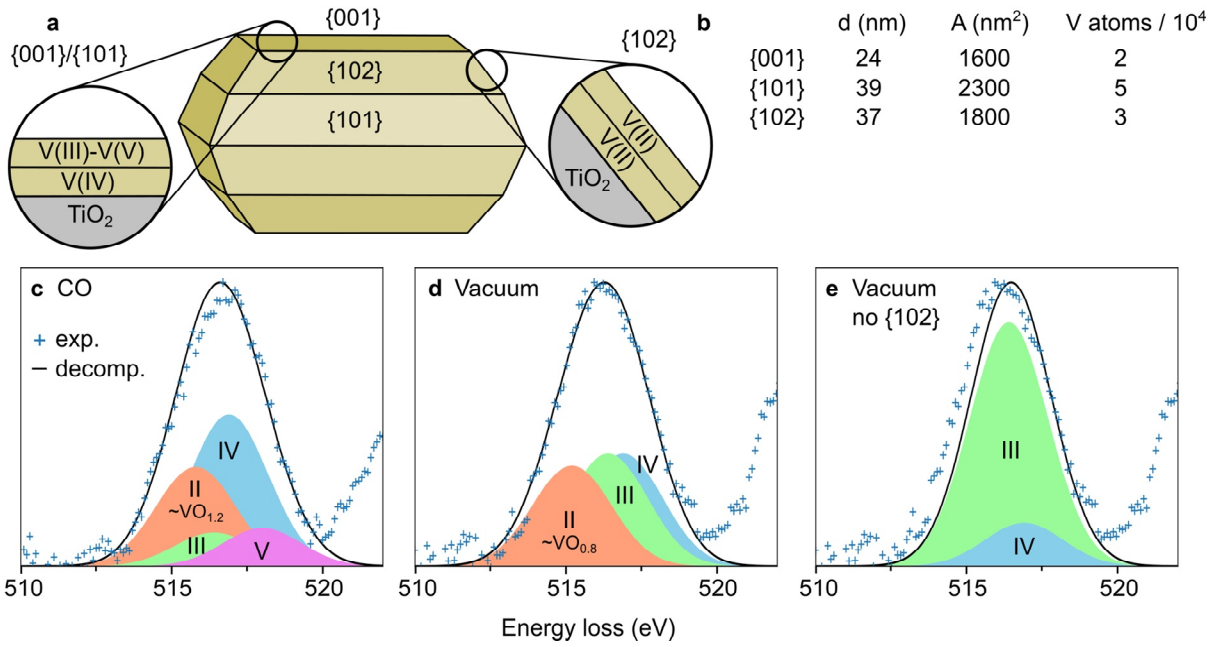

Supplementary Figure S3. Decomposition of EEL spectra into V(II)-V(V) components. (**a**) Average shape of the VO_x-TiO_2 particles (see Supplementary Figure S1) used in the subsequent decompositions, together with the possible oxidation states for each of the two layers of VO_x (see Supplementary Figure S2). (**b**) Calculated areas and number of supported vanadium-atoms for the three facet types included in the model. The number of vanadium atoms is calculated based on bulk truncations of the anatase structure (see main text for the densities used). Note that the {102} facets contribute vanadium atoms at the same order of magnitude as the low-index facets in this model. (**c**-**d**) Modelling of the EEL spectra recorded during (**c**) CO reduction and (**d**) vacuum reduction, which reasonably accounts for the data; these correspond to V/IV/III/II fractions of (**c**) 12/47/11/30 and (**d**) 0/35/35/30, respectively. (**e**) Assuming an absence of {102}, and therefore V(II), in the model clearly leads to an unsatisfactory fit to the experimental data for vacuum reduction. The vanadium reference states are chosen according to the description in ref. [20] in the main text and are each modelled as a Gaussian function with σ= 1.3 eV (based on the narrowest V-L_3 shape measured in the fully oxidized state) and centred according to: V(V) at 518.0 eV, V(IV) at 516.9 eV, V(III) at 516.4 eV. The reference state for V(II) is adapted from Su et al.[28] (515.5 eV) and extrapolated to values for $VO_{1.2}$

(515.8 eV, CO reduction) and $VO_{0.8}$ (515.2 eV, vacuum reduction) assuming a linear shift in energy with oxidation state. These decompositions show the consistency between the TEM images, EEL spectra, and nanoparticle model. Furthermore, the decomposition shows the necessity of (1) including a fraction of high-index facets with V(II) states comparable to the fraction of the low-index facets, (2) retaining V as V(IV)-V(V) during CO reduction, and (3) tuning the V(II) reference between "$VO_{1.2}$" for CO and "$VO_{0.8}$" for vacuum reduction. The estimated V/IV/III/II fractions are, however, uncertain due to: (i) uncertainties in the background subtraction for the experimental EEL spectra, (ii) uncertain fractions of the different facet types, (iii) uncertain energy losses for the reference states, (iv) relatively large σ compared to the energy shifts between the reference states, and (v) the low signal from the 2D VO_x phase.